MEASUREMENTS OF *EUGLENA* MOTION PARAMETERS BY LASER LIGHT SCATTERING

C. ASCOLI, M. BARBI, C. FREDIANI, AND A. MURÈ, *Laboratorio per lo Studio delle Proprietà Fisiche di Biomolecole e Cellule, C.N.R., Pisa, Italy*

ABSTRACT Measurements of *Euglena gracilis* motion parameters have been performed by the spectral analysis of the scattered laser light. Samples were oriented by a radiofrequency field to obtain easily interpretable spectra. Cell rotation frequency and flagellar beating frequency distributions were obtained from the homodyne spectra, whereas the Doppler lines obtained at small observation angles by heterodyne detection yielded the swimming speed distributions. We discuss the broadening of the heterodyne spectra at large angles of observation.

An application of this method to the study of the photo-kinetic effect is also described.

INTRODUCTION

The spectral analysis of laser light scattered from moving particles is a useful tool for measuring the parameters of motion of the particles. Most of the experiments reported in the literature have been performed on biological molecules undergoing diffusion in solution (Brownian motion); a complete bibliography on the topic is given by Cummins and Pusey (1977).

This technique has been extended to the study of more complex systems such as bacteria motions, spermatozoa motility, chemotactic responses of bacteria, protoplasmic streamings, etc. (Berge et al., 1967; Nossal, 1971; Nossal et al., 1971; Nossal and Chen, 1972*a*; Nossal and Chen, 1972*b*; Bergè and Dubois, 1973; Schaefer et al., 1974; Mustacich and Ware, 1974; Boon et al., 1974; Schaefer and Berne, 1975; Banks et al., 1975; Stock, 1976; Mustacich and Ware, 1976; Shimizu and Matsumoto, 1977).

The theory generally used to interpret the experimental results is founded on the hypothesis that the dimensions of the particles are of the same order as, or less than, the laser wavelength and that the particle orientation is statistically independent of its translation (Cummins and Swinney, 1970); a theory of axial and off-axial translatory motion has been developed (Berne and Nossal, 1974) for axial symmetric particles (bacteria) of a size comparable with the laser wavelength.

We used this technique to measure the motion parameters of *Euglena gracilis* (*E.g.*), a flagellated alga largely studied for its response to light stimuli (phototaxis). Unfortunately, *E.g.* has an ellipsoidal shape, and its dimensions are much larger than the laser wavelength. It also executes a complex rototranslatory motion. So the theoretical approach generally adopted in the literature is inapplicable in this case. A thorough analytical treatment of quasi-elastic light scattering from *E.g.* cultures

appears to be very difficult given our inadequate knowledge of the motion and optical properties of the *Euglena* body. Experiments on specimens with similar features (spermatozoa) performed by Bergè and Dubois (1973) have gone no further than to show that the bandwidth of the light beating spectrum increases as sperm motility increases. Dubois et al. (1975), simplifying the complicated motion of spermatozoa to the motion of point scatterers, develop a theoretical approach that allows them to extract the distribution of swimming speeds of human spermatozoa. They do not analyze the complications of orientation dependence, flagellar beating, or multiple scattering. Even so, their results seem to be in good agreement with the measurements obtained by other methods. Their approach provides a relatively simple method of rapidly performing clinically applicable motility assays.

In our experiments we have chosen an experimental approach which, separating the different effects due to the complex rototranslatory motion of the *Euglenas,* made possible the measurement of *E.g.* motion parameters (Ascoli et al., 1971). These favorable experimental conditions (unidirectional motion, appropriate scattering angles) were obtained by exploiting a qualitative knowledge of *E.g.* motion and of the angular distribution of the scattered light intensity, and by using the *Euglena* orientation feature in an alternating electric field; (Teixeira-Pinto et al., 1960; Griffin and Stowell, 1966; Ascoli et al., 1978). A similar experimental approach was followed by Dubois et al. (1974) in measuring the speed distribution of human spermatozoa moving in capillary tubes filled with cervical mucus.

In our experiments the speed of oriented *Euglenas* was measured by analyzing the Doppler shift of the scattered light, whereas body rotation and flagellar beating frequency distributions were obtained by measurements of intensity modulations.

An application of this method to the study of the photokinetic effect on *E.g.* samples is described.

METHODS

Euglena gracilis samples were drawn from a continuous culture, where the cells were grown at 24°C in an autotrophic medium (Cramer and Myers, 1952) with a constant illumination of 3000 lux. The medium was aerated by a mixture of air and 5% CO_2. The samples were placed in a chamber 15 × 15 × 0.2 mm^3 enclosed by two coverglasses 0.17-mm thick. The density of the sample was sufficiently low that only a few cells at a time passed within the laser beam. Fig. 1 shows the experimental set up. To avoid cell sedimentation the chamber containing the sample is placed in a horizontal plane, the laser beam falling on it vertically. The horizontal laser beam coming from the 1 mW He-Ne laser (Spectra-Physics Inc., Mountain View, Calif., model 132; λ_o = 6,328 Å) is split by the semireflecting mirror L_1 into vertical and horizontal beams of the same intensity. The vertical beam falls on the sample placed under L_1; $\mathbf{K}_o$ and $\mathbf{K}_s$ indicate the wave vectors of the incident and scattered light. The scattering plane $\mathbf{K}_o\mathbf{K}_s$ is perpendicular to the direction of the light electric field; the mirror M_1 converts the vertical plane $\mathbf{K}_o\mathbf{K}_s$ into the horizontal plane, where we measure the scattering angles. In Fig. 1 $\mathbf{K}_o'$ and $\mathbf{K}_s'$ indicate the horizontal vectors corresponding to $\mathbf{K}_o$ and $\mathbf{K}_s$. A pin photodiode Ph (HP 5082-4207) generates a photocurrent (containing the beatings between the scattered light and the incident beam) that is then amplified by the 427 Keithley Current Amplifier (Keithley Instruments, Inc., Cleveland, Ohio) and sent to the Federal UA-14A real time analyzer and 1014 averager

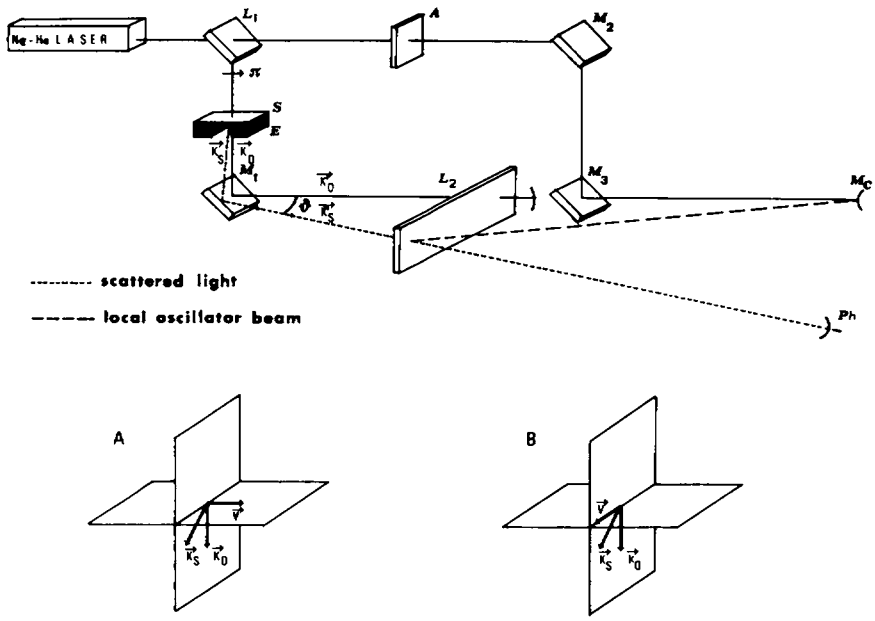

FIGURE 1 Schematic diagram of the heterodyne spectrometer. *S*, sample; *E*, electrodes; M_1, M_2, M_3, plane mirrors; M_c, convex mirror; L_1 and L_2, 50% beam splitters; *A*, attenuator; Ph, photodiode; $\mathbf{K}_o$, $\mathbf{K}_s$, $\mathbf{K}_o'$, $\mathbf{K}_s'$, wave vectors; π, polarization vector. A and B show the two orientations of the cells used in the measurements. The disposition of the electrodes shown in the figure corresponds to the cell orientation of A.

(Federal Systems Group, Syosset, N.Y.). Finally, the output is squared by an analog device and plotted by an *x-y* recorder. Good alignment of the scattered and heterodyning lights is necessary; in fact, if the wave surfaces are not parallel, several interference fringes arise on the detector, reducing the useful signal (Cummins and Swinney, 1970). When we use homodyne detection, the unperturbed beam is simply suppressed.

To obtain a given direction of swimming, a radiofrequency field was applied to the sample. The electrodes used to apply the orienting field were placed under the chamber containing the sample. The 2-MHz field orients the cells parallel to the field (Ascoli et al., 1978). To achieve a good orientation by using low field intensities, the cells were suspended in a medium with a low electrical conductivity ($\sim 10^{-3}$ mho/m); no damage to the cells was observed. We used the two directions of orientation shown in Fig. 1 A and B. In case A the cell orientation—and the swimming direction—were perpendicular to the plane $\mathbf{K}_o\mathbf{K}_s$, whereas in case B they were in the plane $\mathbf{K}_o\mathbf{K}_s$ and perpendicular to $\mathbf{K}_o$. This last orientation was obtained by rotating the electrodes at right angles to the position represented in Fig. 1.

EUGLENA GRACILIS FEATURES

Euglena gracilis is an elongated protozoan whose dimensions are about 60, 10, and 10 μm. Its propulsion is supplied by a long flagellum beating around the body. *Euglena gracilis (E.g.)*, like the *Euglena viridis* studied by Lowndes (1941), moves with a translation speed v of about 100 μm/s; its body is slightly inclined all the time with respect to the axis of translation and rotates around this. The *E.g.* motion is schematically

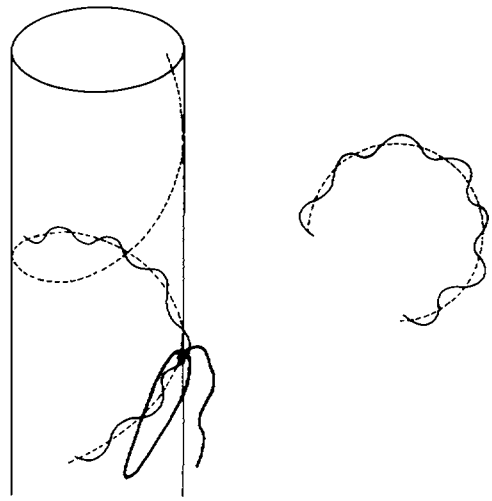

FIGURE 2 Schematic drawing of *E.g.* motion. The *inset* shows the path traced out by the anterior end of the cell on a plane perpendicular to the direction of motion.

shown in Fig. 2. The rotation frequency, as estimated by microscopic observations, is about 2 Hz. The flagellar beating causes the front of the body to oscillate during its almost helicoidal motion (see Fig. 2, *inset*).

The *E.g.* motion is affected by light but phototactic phenomena are negligible at the wavelength of the laser light (Wolken, 1967). In the absence of external stimuli the translation velocity v is constant over lengths > 1 mm.

Euglena gracilis, like other microrganisms (Teixeira-Pinto et al., 1960), can be oriented by applying a radiofrequency field. This orientation, which is due to a passive electrical mechanism (Ascoli et al., 1978), is parallel or perpendicular to the direction of the electric field, according to its frequency (Griffin and Stowell, 1966). The perpendicular orientation allows the cell to move in any direction in the plane perpendicular to the field, whereas the parallel orientation only allows motion in the direction of the field; so, to have a bidirectional motion, we used the parallel orientation.

The *Euglena* motion parameters are affected by the field (Ascoli et al., 1978) but we found it possible to orient *Euglena* cells without causing significant kinematic changes, by using fields of fairly low intensity.

INTENSITY DISTRIBUTION OF THE SCATTERED LIGHT

The intensity of the light scattered from an *E.g.* cell placed under the 1-mW laser beam is enough to allow it to be directly observed on a screen. The intensity distribution of the light scattered from *E.g.* cells turns out to be markedly nonuniform. Photograms of the light scattered from living *E.g.* cells are reported in Fig. 3. The chamber containing the sample was placed at right angles to the laser beam, and the film was fixed about 20 cm from the sample in the plane perpendicular to the laser beam. Fig. 3*a* shows the light scattered from three cells swimming in different directions. Fig. 3*b*

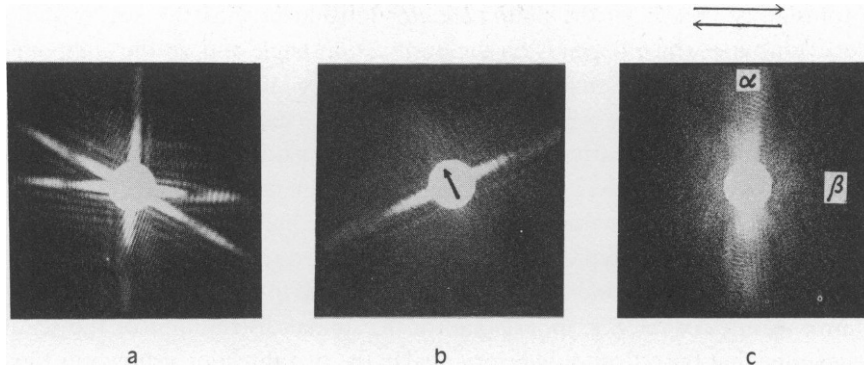

FIGURE 3 Light scattering patterns from *Euglena:* (a) unoriented cells; (b) single cell; (c) oriented cells. The arrows indicate the direction of the orienting field. α is the position of the photodetector chosen to reveal the intensity modulations of the scattered light; β is the photodetector position chosen to reveal the Doppler shift of the scattered light. In all the pictures, the white spot masks the image of the direct laser beam.

shows the scattering pattern from a single cell swimming through the laser beam in the direction shown by the arrow. The light scattered from the cell appears to be nonuniformly distributed around the laser beam, with a sharp intensity peak at right angles to the major axis of the cell. If the light scattered from an *E.g.* cell is observed on a screen, this peak appears to oscillate to some degree around the laser beam; this is due to the rotation of the cell's longest axis around the translation direction. Fig. 3 *c* shows the scattering pattern for *E.g.* samples oriented by the radiofrequency field. The broader intensity peak of the light scattered at right angles to the direction of motion (shown by the arrows) is due to the addition of the individual intensity peaks of cells with the same swimming direction but different phases of rotation.

Clearly, the oscillation of the individual intensity peaks will produce a modulation of the light intensity detected at a given point; the modulation will be greatest when the photodetector is placed near the peak (for instance at α in Fig. 3 *c*), whereas negligible intensity modulation will be detected when the detector is in the almost uniform region of the light scattering pattern (at β in Fig. 3 *c*). Photodetector positions α and β are created by the cell orientation of A and B, respectively, in Fig. 1.

EXPERIMENTAL APPROACH AND RESULTS

When a monochromatic plane wave of frequency ν^* and wave vector $\mathbf{K}_o$ polarized at right angles to the scattering plane falls on a point scatterer, the field scattered in a given direction is expressed (Cummins and Swinney, 1970) by:

$$E_s = A e^{-j[2\pi\nu^* t - (\mathbf{K}_o - \mathbf{k}_s)\cdot\mathbf{r}(t)]}$$

where $\mathbf{K}_s$ is the wave vector of the scattered field and $\mathbf{r}(t)$ is the time dependent vector giving the position of the scatterer. Let $\mathbf{q} = \mathbf{K}_o - \mathbf{K}_s$; the assumption $K_s \simeq K_o = 2\pi/\lambda_o$ yields $q = 2K_o \sin \theta/2$ where $\theta = {}_{\mathbf{K}_o\mathbf{K}_s}$ is the observation angle. Thus, uni-

form translatory motion of the point scatterer introduces into the scattered field a frequency shift $\mathbf{q}\cdot\mathbf{v}$ which depends on the observation angle and on the component of the velocity $\mathbf{v}$ in the $\mathbf{q}$ direction (Doppler effect). But *E.g.* cells are not point scatterers, and they move in a complex way. Therefore it must be expected that both the amplitude and the phase of the scattered field will be time-dependent in a way determined by the geometry of the cell body, its orientation, and motion parameters.

To measure *E.g.* motion parameters by analyzing the light scattered from swimming cells, we have worked on samples oriented by a radiofrequency field (see Methods), so that cells of the same shape and size scatter the same light intensity on the detector. The qualitative features of the *E.g.* motion and of the spatial distribution of the scattered light suggested that the cells should be oriented in the two directions shown in Fig. 1 A and B.

Intensity Modulations

In the case illustrated in Fig. 1 A, the translational velocity $\mathbf{v}$ of the oriented cells is perpendicular to the plane $\mathbf{K}_o\mathbf{K}_s$. The detector, as if it were at α in Fig. 3 *c*, is in a suitable position to reveal the intensity modulations of the scattered light. In this case, in fact, the Doppler shift vanishes ($\mathbf{v}$ is perpendicular to $\mathbf{K}_o$ and to $\mathbf{K}_s$) and the photocell detects the periodically oscillating light peak (see above). We will then expect that the amplitude of the field scattered by a single *Euglena* will vary periodically in time, as the orientation of the cellular body does; the period of this amplitude modulation is the period of the cell rotation around the axis of motion, so that it does not depend on the angle of observation or the other motion parameters.

When the photodetector receives the scattered light (homodyne detection), a photocurrent is set up:

$$i(t)\,\alpha\,E_s(t)E_s^*(t) = \sum_1^N A_k^2(t) + \begin{array}{l}\text{cross terms between the fields}\\ \text{scattered from different } \textit{Euglenas},\end{array}$$

where $A_k(t)$ is the amplitude of the field scattered from the k^{th} *Euglena*, and N is the number of the cells under the laser beam. The beating terms can be neglected as long as N is not too high. In our experiments, N is about $5 \div 10$ and therefore we expect that in homodyne detection the spectral line due to the first term will appear very clearly. This line should be at the rotation frequency whatever the angle of observation. We also neglect the term due to the fluctuations in number that, as Schaefer and Berne (1972) have shown, occur when the number of the cells under the laser beam is very small ($\overline{N} \simeq 1$). This term, in fact, makes a distributed contribution to the spectrum, and this contribution does not significantly modify the intensity modulation lines. Lastly, in this experimental arrangement, the translatory velocity $\mathbf{v}$ is perpendicular to the scattering plane and thus no Doppler effect can occur.

Figs. 4 and 5 show two spectral lines obtained by homodyne detection with this experimental arrangement; they are centered at 1.8 and 40 Hz, respectively, and, as expected, do not depend on the angle of observation (compare Figs. 4 and 5). The 1.8 Hz line, in agreement with microscope observation, is due to the cell rotation, whereas we

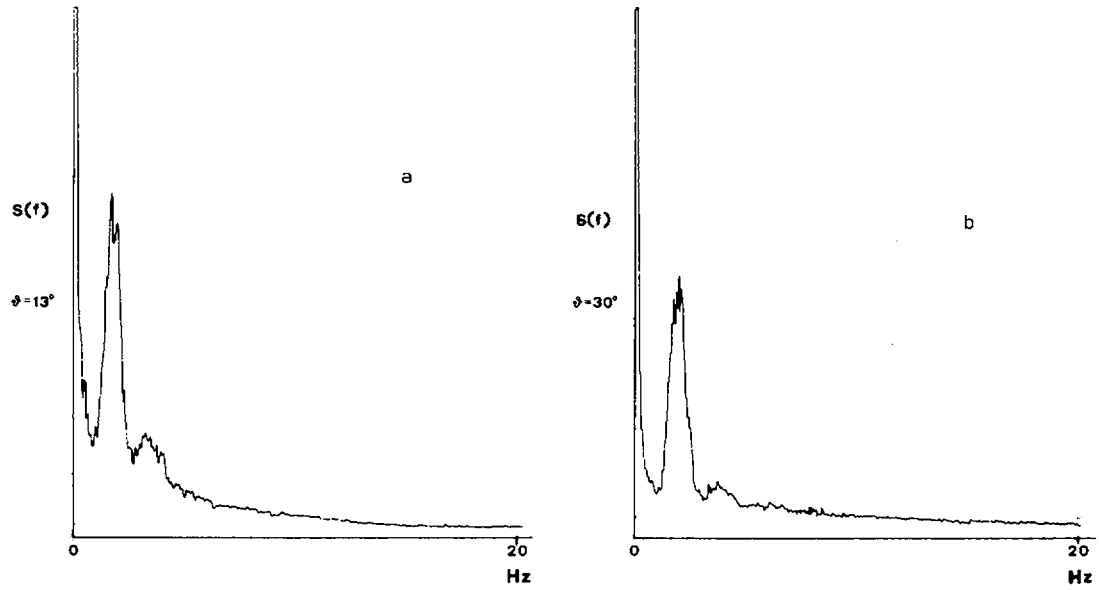

FIGURE 4 Homodyne spectra showing the light intensity modulation due to the rotation of *Euglena*, for two values of ϑ. The cells are moving with v perpendicular to the scattering plane.

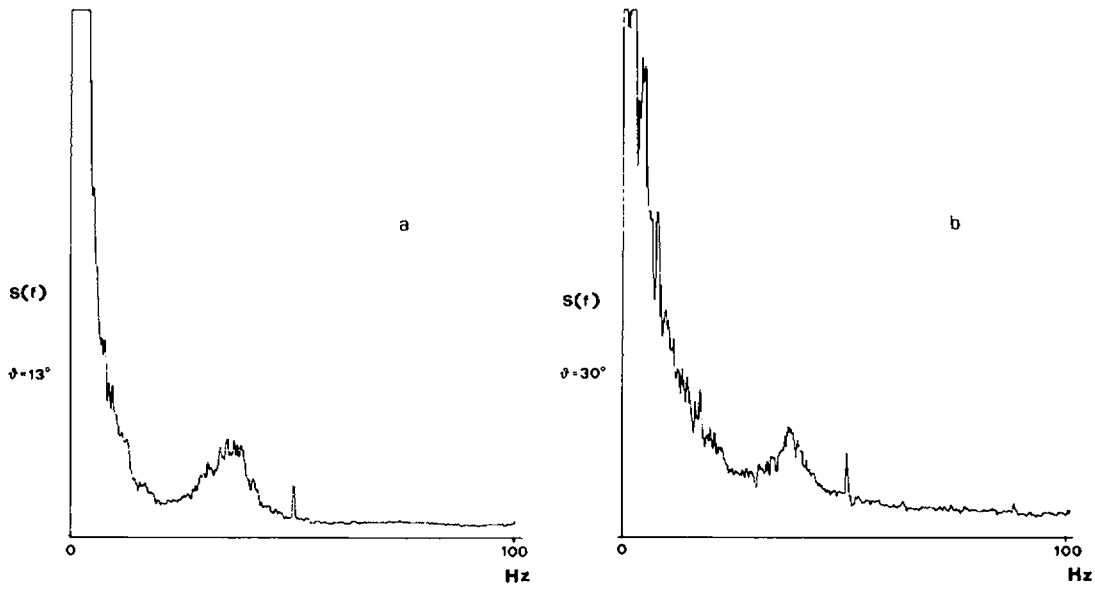

FIGURE 5 Homodyne spectra showing the light intensity modulation due to the flagellar beating of *Euglena*. Same sample as in Fig. 4 but different scales for abscissas and ordinates.

ascribe the 40-Hz line to body vibrations associated with the flagellar beating (Lowndes, 1941). A line at twice the body rotation frequency usually appears also (Fig. 4).

Velocity Measurements

To determine the velocity of *Euglenas* from the Doppler shift of scattered laser light, the cells were oriented in the scattering plane (as in Fig. 1 B). In this case $\mathbf{K}_o$, $\mathbf{K}_s$, and $\mathbf{v}$ are in the same plane, and $\mathbf{v}$ is perpendicular to $\mathbf{K}_o$. The photodetector (as at β in Fig. 3 *c*) collects light belonging to the almost uniform region of the scattering pattern of each *Euglena;* so the intensity of the light falling on the photodetector will be almost constant in time. This is confirmed by Fig. 6, showing homodyne spectra obtained from the same samples of Figs. 4 and 5 but with $\mathbf{v}$ in the $\mathbf{K}_o\mathbf{K}_s$ plane. It may be seen that the 1.8-Hz line vanishes and that the 40-Hz line is greatly reduced.

It is now necessary to make some assumptions in order to interpret our experimental results. We will suppose that all the cells are identical in shape and size and that they therefore scatter the same light intensity on the photodetector. Moreover we will treat the *E.g.* motion as a helicoidal motion, so that all the points in the cell body follow helicoidal pathways with the same radius. This is only a first approach to an analytical treatment of the field scattered from *E.g.* cells, but, as shown below, it is able to interpret the experimental results.

Let us call $\mathbf{r}_P(t)$ the vector giving the time-dependent position of a generic point P in the cell body of a *Euglena*. For a helicoidal motion we can write:

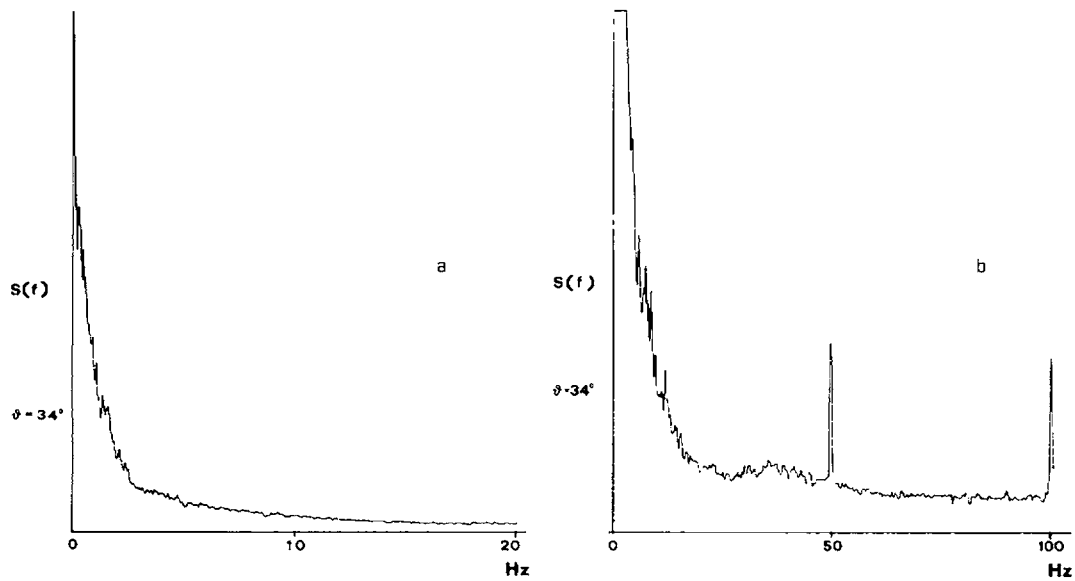

FIGURE 6 Homodyne spectra for *Euglena* moving with $\mathbf{v}$ in the scattering plane and perpendicular to the laser beam. Light intensity modulations are strongly reduced.

$$\mathbf{r}_P(t) = \mathbf{r}_P^0 + \mathbf{r}(t), \tag{1}$$

where $\mathbf{r}(t)$ is equal for all the points in the cell. Then the field E scattered from a single *Euglena* on the photodetector is:

$$E = Ae^{-j(2\pi\nu^* t - \mathbf{q}\cdot\mathbf{r}(t) + \varphi_o)}, \tag{2}$$

where φ_o is a suitable time-independent phase factor and A, which is equal for all the oriented cells and constant in time, is the amplitude of the scattered field. Now, by choosing the axis in the same direction as $\mathbf{K}_o$ and the z axis in the $\mathbf{K}_o\mathbf{K}_s$ plane at an acute angle with $\mathbf{K}_s$, we can write:

$$\begin{aligned} r_x &= a \sin 2\pi\nu_r t & q_x &= q \sin(\vartheta/2) = (4\pi/\lambda_o)\sin^2(\vartheta/2) \\ r_y &= \mp a \cos 2\pi\nu_r t & q_y &= 0 \\ r_z &= \pm vt & q_z &= -q\cos(\vartheta/2) = -(2\pi/\lambda_o)\sin\vartheta. \end{aligned} \tag{3}$$

The upper and lower signs hold for *Euglenas* moving forward or backward, respectively; ν_r is the rotation frequency and a the radius of the helicoidal path. So we have:

$$E = Ae^{-j(2\pi\nu^* t - q_x \sin 2\pi\nu_r t \mp q_z vt + \varphi_o)} \tag{4}$$

This is the typical form of a frequency modulated signal. It can be shown (Lathi, 1968) that such a signal has significant spectral components in a band of finite width. To obtain the spectrum of E we may use the mathematical identity:

$$e^{jq_x a \sin 2\pi\nu_r t} = \sum_{n=-\infty}^{+\infty} J_n(q_x a) e^{+jn2\pi\nu_r t}, \tag{5}$$

where the J_n are the Bessel functions of the first kind. Then we have, omitting the non-essential factor $e^{-j\varphi_o}$:

$$\begin{aligned} E &= Ae^{-j(2\pi\nu^* \mp q_z v)t} \sum_{n=-\infty}^{+\infty} J_n(q_x a) e^{jn2\pi\nu_r t} = \\ &= Ae^{-j2\pi[\nu^* \pm (v/\lambda_o)\sin\vartheta]t} \sum_{n=-\infty}^{\infty} J_n[4\pi(a/\lambda_o \sin^2(\vartheta/2)] \quad e^{j2\pi n\nu_r t}. \end{aligned} \tag{6}$$

Thus the field scattered from a forward swimming *Euglena* has components at the frequencies

$$\nu_n = \nu^* + (v/\lambda_o)\sin\vartheta \pm n\nu_r, \text{ (n positive or negative integer).} \tag{7}$$

The central component at the frequency $\nu_o = \nu^* + (v/\lambda_o)\sin\vartheta$ corresponds to the Doppler shift caused by the swimming speed v, whereas the lateral lines, which show a shift of ν_r or its multiples, are produced by the rotation of the cell around its axis of motion. For the power spectrum of E, Eq. 6 yields:

$$T(\nu) = A^2 \sum_{n=-\infty}^{+\infty} J_n^2[4\pi(a/\lambda_o)\sin^2(\vartheta/2)]\,\delta(\nu - \nu_n) \tag{8}$$

$T(\nu)$ is symmetric around ν_o, because $J_{-n}(x) = (-)^n J_n(x)$. Table I gives $J_n^2(q_x a)$ for $\vartheta = 2°$ and $\vartheta = 20°$, assuming the parameter a is equal to 5 and 10 μm, respectively. For $\vartheta = 2°$ only the central component, which is at the Doppler frequency, is present, whereas for $\vartheta = 20°$ significant lateral lines in a band of half width $4\nu_r$ or $7\nu_r$, depending on the a value, are found.

Given the statistical independence of the cells, the optical spectrum of the light scattered by a population of *Euglenas* is the sum of the individual spectra $T(\nu)$. It will be made up of two bands of identical shape symmetrically placed on either side of ν^*, given the equal probability of the two possible directions of motion. At small angles of observation($q_x a = 4\pi/\lambda_o \sin^2 \vartheta/2 \ll 1$) only the components at the Doppler frequencies will be present. The optical spectrum can be revealed by heterodyne detection and by performing a spectral analysis of the photocurrent. In fact, the photocurrent power spectrum, in heterodyne detection, reproduces the superposition of the right and left bands of the optical spectrum at low frequencies and its components occur at the frequencies $f_n = |\nu_n - \nu^*| = (v/\lambda_o)\sin\vartheta + n\nu_r$ (n positive or negative integer). At small angles it will then be homologous to the distribution of the *Euglenas* swimming speeds according to the linear relation

$$f_o = (v/\lambda_o)\sin\vartheta. \tag{9}$$

Instead, at large observation angles, the line is not only due to the translation but also to the rotation of the cell body, which produces a frequency modulation of the scattered field. At large ϑ the spectrum can be deduced from the spectrum at small ϑ. Let us call $G(f_o)df_o$ the number of scatterers with Doppler shift between f_o and $f_o + df_o$, so that $G(f_o)$ is homologous to the speed distribution through Eq. 9. The spectrum

TABLE I
$J_n^2(q_x a)$ VALUES

	$a = 5\,\mu$m			$a = 10\,\mu$m	
	ϑ			ϑ	
n	2°	20°	n	2°	20°
0	0.9984	0.0666	0	0.9969	0.0216
1	$2.28\,10^{-4}$	0.1169	1	$9.12\,10^{-4}$	0.0776
2	—	0.2362	2	—	0.0576
3	—	0.0942	3	—	0.0139
4	—	0.0170	4	—	0.1290
5	—	$1.85\,10^{-3}$	5	—	0.1303
6	—	$1.3\,10^{-4}$	6	—	0.0595
7	—	—	7	—	0.0164
			8	—	$3.1\,10^{-4}$
			9	—	$4.3\,10^{-4}$

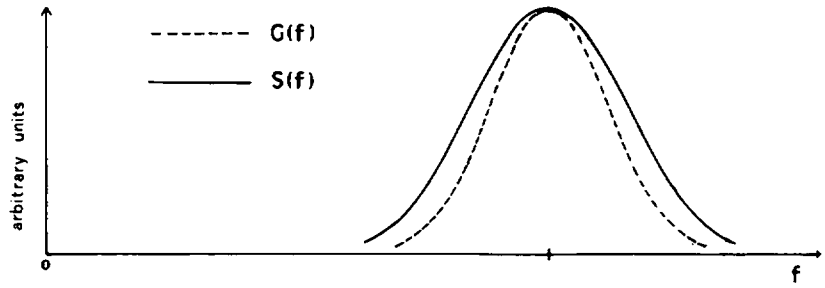

FIGURE 7 Normalized functions $G(f)$ and $S(f)$. $G(f)$ (dotted line) is the Gaussian function interpolating the Doppler line of Fig. 8 *a*. Mean speed 122 μm/s; fractional line width 0.14. $S(f)$ (continuous line) is the function calculated according to Eq. 10 for $\vartheta = 20°$ and for $a = 7$ μm.

$S(f)$ at large ϑ is then given by the convolution integral

$$S(f) = \int_0^{\infty} W(f - f_o)\, G(f_o)\, df_o, \tag{10}$$

where $W(f - f_o) = A \sum_{n=-\infty}^{+\infty} J_n^2(q_x a)\delta(f - f_o - n\nu_r)$ is the spectral distribution for a scattering cell with Doppler shift f_o. By using the suitable J_n^2 values and assuming a Gaussian distribution for $G(f)$, we have computed the integral (Eq. 10) numerically. Fig. 7 shows $G(f)$ and $S(f)$ for $\vartheta = 20°$ and $a = 7$ μm. The mean value of the speeds and their standard deviation, as well as the Gaussian shape of $G(f)$, were chosen in agreement with the experimental data reported below. As may be seen from Fig. 7, up to 20° the frequency modulation introduces only slight change in the shape, and a small enlargement, of $S(f)$ with respect to $G(f)$.

This theoretical analysis may now be compared with the experimental results. Fig. 8 shows the spectra obtained from the same sample for $\vartheta = 2°$ and $\vartheta = 20°$. These

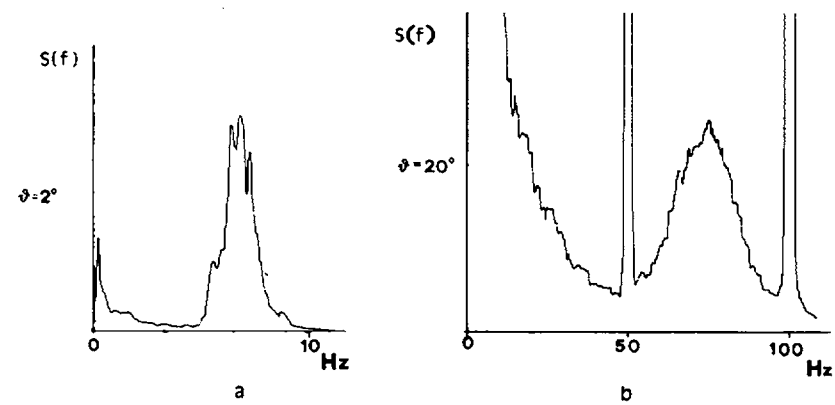

FIGURE 8 Heterodyne spectra showing Doppler lines for small and large scattering angle; the cells are moving with v in the scattering plane and perpendicular to the laser beam. Here, as in other reported spectra, sharp peaks due to the ripple appear at the line frequency (50 Hz) and its multiples. They are useful as frquency markers.

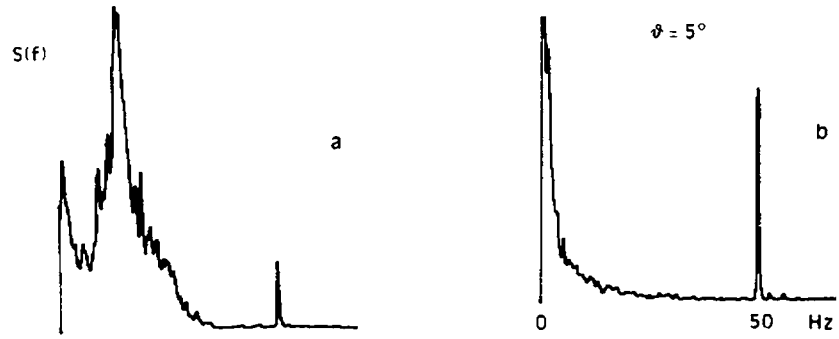

FIGURE 9 Comparison between the heterodyne spectra of the light scattered from (a) living cells and (b) cells killed by warming the sample at 60°C. In b the amplification is four times that of a. Different sample from Fig. 8.

spectra show a line superimposed on a zero frequency band; the line position, its width, and that of the zero-centered band depend on the observation angle. For samples of dead *Euglenas* the line disappears and the band is greatly reduced (Fig. 9). The band is different for different samples and appears to be caused mainly by anomalously moving cells. At times, in fact, some of the cells stop, but continue to wiggle, giving a zero-centered contribution to the spectrum. On the other hand, the line is related to the oriented motion, as is confirmed by plotting the frequency of the maximum of the spectral lines for the sample of Fig. 8 against sin ϑ (Fig. 10*a*). Considering the amount of time needed to carry out the measurements at several angles and the consequent changes in the sample, the experimental points do, in fact, show a good fit with the linear relation (9). The straight line interpolating the experimental points in Fig. 10*a*

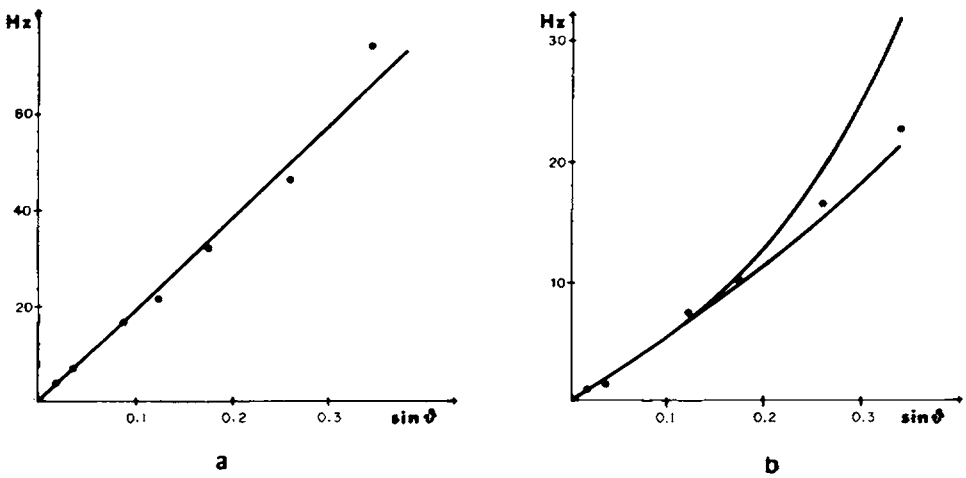

FIGURE 10 (a) Doppler shift due to the translation motion of *Euglenas* as a function of sin ϑ; (b) line width against sin ϑ. The curves are calculated by Eq. 10 for $a = 5$ μm (dotted line) and for $a = 10$ μm (continuous line). Data obtained from the same sample as in Fig. 8.

corresponds to a swimming speed of 122 μm/s; experiments with different samples gave values in the range 80–400 μm/s. In Fig. 10*b* we report the half-height line width against sin ϑ. The two curves reported together with the experimental points are the plot of the theoretical line widths against sin ϑ for $a = 5$ and 10 μm, respectively, and for a swimming speed distribution with a fractional line width of 0.14. We see that a cannot exceed 10 μm, the most likely value being about 7 μm. For a correct interpretation of this result, we must recall that the motion of *E.g.* is more complex than we have assumed here. While the cell is swimming, its longest axis is at all times inclined at about 10° to the axis of motion and the cellular body rotates, with the same side always facing the axis of motion. So different points of the cell follow helicoidal pathways of different radii and give different contributions to the lateral bands. The number and weight of the lateral bands corresponding to any given point will depend on its distance from the axis of rotation (and on geometrical factors, too). Even so, all the bands are far from the Doppler frequency of ν, or its multiples. Thus, the lateral bands, which occur in the optical spectrum $T(\nu)$ of a single *Euglena*, are the result of the superposition of the correlated bands corresponding to the different points of the cell. So the experimental spectra only yield a crude estimate of the mean radius of the helicoidal pathways described by the *Euglenas*.

CONCLUDING REMARKS

Our results show that the technique of orienting the *Euglena* cells simplifies the study of their complex motion.

An *E.g.* cell has a nonuniform light scattering pattern, with a sharp peak in the plane perpendicular to the major axis of the cell; the rotation of the cell around the direction of travel makes this peak oscillate periodically. In oriented samples, all the oscillating peaks are superimposed; by placing the photo-detector near these (as at α in Fig. 3*c*) in homodyne detection, the intensity modulation of the scattered light was measured, thus giving the distributions of the rotation frequency and flagellar beating frequency.

To measure the phase shift of the scattered light induced by the Doppler effect, we used heterodyne detection, placing the photodetector in the almost uniform region of the scattering pattern (as at β in Fig. 3*c*); with this experimental arrangement the Doppler shift mainly depends on the translatory motion of the cell. For large observation angles, the rotatory component of the motion should produce an enlargement of the heterodyne spectra. Our results show that this enlargement is actually very small for observation angles up to 20°.

Thus, all the motion parameters (swimming speed, rotation frequency, and flagellar beating frequency) can be measured by choosing suitable experimental conditions and detection methods. As quantitative measurements of motion parameters can be carried out in only a few minutes, this method can be used to investigate biological effects in *Euglena* and other microorganisms. As an example, we will now report the preliminary results of an experiment on the effect of white light on the motion parameters of oriented *Euglenas*. Fig. 11 shows the spectra obtained from a dark-adapted sample after three successive exposures to 10,000 lux of white light. In this sample, which had

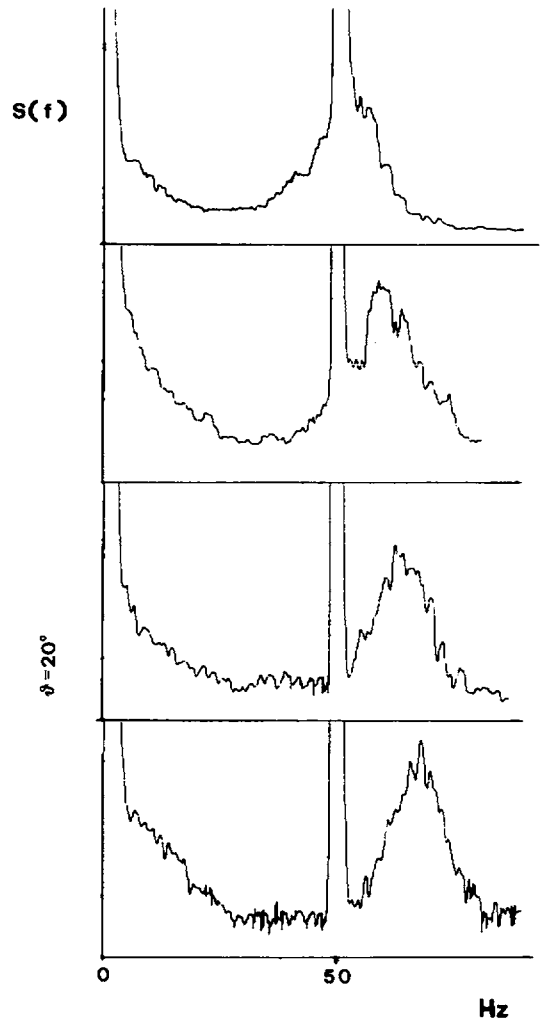

FIGURE 11 Spectra showing the increase in swimming speeds of *Euglenas* by photokinesis. 50 Hz correspond to 92.5 μ/s.

been kept in the dark for several hours, the mean speed increased from 98 μm/s to 126 μm/s after about $\frac{1}{2}$-h exposure to light. In the same sample we also observed the increase in body rotation and flagellar beating frequencies. This method could, therefore, also be used to investigate the relation between the different motion parameters. Another application of the method (the study of the electrokinetic effect of the orienting radiofrequency field) is given in the companion paper (Ascoli et al., 1978).

We thank G. Del Carratore and M. Torti for supplying *Euglena* cultures. We are grateful to L. Vanni for his assistance in setting up the electronics.

Received for publication 20 March 1978.

REFERENCES

ASCOLI, C., M. BARBI, C. FREDIANI, and D. PETRACCHI. 1978. Effects of electromagnetic field on the motion of *Euglena gracilis*. *Biophys. J.* **24**:601.

ASCOLI, C., M. BARBI, C. FREDIANI, D. PETRACCHI, and C. TRIMARCO. 1971. Osservazioni sul moto di Euglena Gracilis mediante diffusione di luce laser. Atti del Congresso di Cinernetica. Casciana Terme. 11–13 October 1971. 296.

BANKS, G., D. W. SCHAEFER, and S. S. ALBERT. 1975. Light scattering study of temperature dependence of *Escherichia coli* motility. *Biophys. J.* **15**:253.

BERGÈ, P., and M. DUBOIS. 1973. Dispositif de mesures optiques adapté a l'étude du mouvement de microorganismes vivants. *Rev. Phys. Appl.* **8**:89.

BERGÈ, P., B. VOLOCHINE, R. BILLARD, and A. HAMELIN. 1967. Mise en évidence du mouvement propre de micro-organismes vivants grace à l'étude de la diffusion inélastique de la lumière. *C. R. Acad. Sci. Paris.* **D265**:889.

BERNE B. J., and R. NOSSAL. 1974. Inelastic light scattering by large structured particles. *Biophys. J.* **14**: 865.

BOON, J. P., R. NOSSAL, and S. H. CHEN. 1974. Light scattering spectrum due to wiggling motions of bacteria. *Biophys. J.* **14**:847.

CRAMER, M., and J. MYERS. 1952. Growth and photosynthetic characteristics of *Euglena gracilis*. *Arch. Mikrobiol.* **17**:384.

CUMMINS, H. Z., and P. N. PUSEY. 1977. Dynamics of Macromolecular Motion in Photocorrelation Spectroscopy and Velocimetry. H. Z. Cummins and E. R. Pike, editors. Plenum Publishing Corp., New York. 164.

CUMMINS, H. Z., and H. L. SWINNEY. 1970. Light Beating Spectroscopy in Progress in Optics. Vol. 8. E. Wolf, editor. North-Holland Publishing Co., Amsterdam. 135.

DUBOIS, M., P. JOUANNET, P. BERGÈ, and G. DAVID. 1974. Spermatozoa motility in human cervical mucus. *Nature (Lond.).* **252**:711.

DUBOIS, M., P. JOUANNET, P. BERGÈ, B. VOLOCHINE, C. SERRES, and G. DAVID. 1975. Methode et appareillage de mesure objective de la mobilité des spermatozoides humains. *Ann. Phys. Biol. Med.* **9**:19.

GRIFFIN, J. L., and R. E. STOWELL. 1966. Orientation of *Euglena* by radiofrequency fields. *Exp. Cell Res.* **44**:684.

LATHI, B. P. 1968. Communication Systems. John Wiley & Sons, Inc., New York. 210.

LOWNDES A. G. 1941. On flagellar movement in unicellular organisms. *Proc. Zool. Soc. Lond.* **A111**:111.

MUSTACICH, R. V., and B. R. WARE. 1974. Observation of protoplasmic streaming by laser-light scattering. *Phys. Rev. Lett.* **33**:617.

MUSTACICH, R. V., and B. R. WARE. 1976. A study of protoplasmic streaming in *Nitella* by laser doppler spectroscopy. *Biophys. J.* **16**:373.

NOSSAL, R. 1971. Spectral analysis of laser light scattered from motile microorganisms. *Biophys. J.* **11**:341.

NOSSAL, R., and S. H. CHEN 1972 *a*. Light scattering from motile bacteria. *J. Phys. (Paris).* **33-C1**:171.

NOSSAL, R., and S. H. CHEN. 1972 *b*. Laser measurements of chemotactic response of bacteria. *Opt. Commun.* **5**:117.

NOSSAL, R., S. H. CHEN, and C. C. LAI. 1971. Use of laser scattering for quantitative determinations of bacterial motility. *Opt. Commun.* **4**:35.

SCHAEFER, D. W., G. BANKS, and S. S. ALPERT. 1974. Intensity fluctuation spectroscopy of motile microorganisms. *Nature (Lond.).* **248**:162.

SCHAEFER, D. M., and B. J. BERNE. 1972. Light scattering from non-Gaussian concentration fluctuations. *Phys. Rev. Lett.* **28**:475.

SCHAEFER, D. W., and B. J. BERNE. 1975. Number fluctuation spectroscopy of motile microorganisms. *Biophys. J.* **15**:785.

SHIMIZU, H., and G. MATSUMOTO. 1977. Light scattering study on motile spermatozoa. *IEEE (Inst. Electr. Electron. Eng.) Biomed. Eng.* **24**:153.

STOCK, G. B. 1976. Application of splines to the calculation of bacterial swimming speed distribution. *Biophys. J.* **16**:535.

TEIXEIRA-PINTO, A. A., L. J. NEJELSKI, JR., J. L. CUTLER, and J. H. HELLER. 1960. The behavior of unicellular organisms in an electromagnetic field. *Exp. Cell Res.* **20**:548.

WOLKEN, J. J. 1967. Euglena. Meredith Publishing Co., Des Moines, Iowa. 142.